

---

**A. Chatterjee**  
**R. Pratap**

Mechanical Engineering  
Indian Institute of Science  
Bangalore, India

**C. K. Reddy**

Engineering Science and Mechanics  
Virginia Polytechnic Institute and State University  
Blacksburg, VA, USA

**A. Ruina**

Theoretical and Applied Mechanics  
and Mechanical and Aerospace Engineering  
Cornell University, Ithaca, NY, USA

# Persistent Passive Hopping and Juggling is Possible Even With Plastic Collisions

## Abstract

*We describe simple one-dimensional models of passive (no energy input, no control), generally dissipative, vertical hopping and one-ball juggling. The central observation is that internal passive system motions can conspire to eliminate collisions in these systems. For hopping, two point masses are connected by a spring and the lower mass has inelastic collisions with the ground. For juggling, a lower point-mass hand is connected by a spring to the ground and an upper point-mass ball is caught with an inelastic collision and then re-thrown into gravitational free flight. The two systems have identical dynamics. Despite inelastic collisions between non-zero masses, these systems have special symmetric energy-conserving periodic motions where the collision is at zero relative velocity. Additionally, these special periodic motions have a non-zero sized, one-sided region of attraction on the higher-energy side. For either very large or very small mass ratios, the one-sided region of attraction is large. These results persist for mildly non-linear springs and non-constant gravity. Although non-collisional damping destroys the periodic motions, small energy injection makes the periodic motions stable, with a two-sided region of attraction. The existence of such special energy conserving solutions for hopping and juggling points to possibly useful strategies for both animals and robots. The lossless motions are demonstrated with a table-top experiment.*

**KEY WORDS**—hopping robot, juggling robot, passive-dynamic, collisions, efficiency, periodic, map

## 1. Introduction

Two goals for both animals and machines are smooth motion and energy efficiency. Collisions compromise both goals. Thus, collision avoidance is a natural part of much machine design and may be a basic principle in animal locomotion.

For locomotion of animals and machines on level ground, the positive mechanical work needed is equal to the energy losses. With a given actuator efficiency, the energetic efficiency of locomotion can be increased only by reducing energy loss. For terrestrial locomotion, there are losses due to internal viscous-like dissipation, work absorbed by actuators, inelastic ground deformation, and viscous losses in the surrounding fluids. For running and hopping, much of the energy loss is due to motion stoppages and reversals that can be modeled at some level as collisional. Similarly, in the handling of objects that are not lifted a net distance on average, as is stereotyped by juggling, the energy cost comes from the energy losses, some of which are collisional, as when a falling ball is caught with a massive hand.

The second major energy sink is the negative work of actuators. Most actuators used by animals and robots are non-regenerative and work done on the actuator is not recoverable. Additionally, there is usually an energetic cost (electrical, hydraulic, or chemical) associated with absorbing work. Thus, a simple design rule for energetically efficient locomotion and manipulation is that both collisional losses and negative actuator work should be avoided.

One way to reduce collisional loss is to have elastic energy-conserving collisions, and one means to elastic collisions is to eliminate the mass of the contacting points; that is, to have

contact mediated with material that is as close in behavior to a massless spring as possible. This use of springs to conserve energy in collisional interactions, such as in a “Pogo stick,” is the first of Alexander’s (Alexander 1990) “three uses for springs in legged locomotion”. This is one of the two commonly proposed explanations for why the feet of many animals are relatively light (the other is the relative ease of moving a lighter end point from place to place).

However, no foot or juggling hand is actually massless, so some collisional dissipation might seem inevitable. For a given foot mass, the collisional loss can be reduced by reducing the impact velocity. But if this velocity reduction is accomplished by controlled actuation, then the net energy savings could be small or none, because, unless carefully arranged in the context of an overall coordination strategy, this actuation will involve negative work, or will cause positive changes in kinetic energy that will be lost later in the motion (Blajer and Schiehlen 1992).

Alexander’s (Alexander 1990) second use of springs is to speed leg swinging for faster locomotion. Closely related to this function is that springs can aid leg swinging not just to speed up locomotion, but to allow smaller steps at a given speed so as to reduce large collisional losses associated with large stance leg angles (see Kuo (2002)). (Alexander’s third use of springs—to increase the duration of, and thus reduce the forces in, collisional interactions—is not relevant here).

Because collisional interactions or their avoidance seem to be so important in the energetics of legged locomotion, Chatterjee and Garcia (2000) sought to understand the optimal energetic efficiency of certain simple passive-dynamic walking machines built with rigid bodies linked by hinges. They found that zero dissipation per unit distance could only be achieved for these machines in the limit of zero velocity motion. In light of that result, we wondered if finite-speed locomotion could be perfectly efficient if the use of springs were allowed. In this paper, we pursue this idea with a simple model of passive vertical hopping. In particular, we pursue the use of springs to reduce collisional losses in locomotion not by mediating collisional interactions, but by avoiding them. A simple model of “juggling” turns out to have identical governing equations and phenomenology.

## 2. Related Hopping and Juggling Research

The basic phenomenon discussed here—that springs can help conserve energy by passively retracting otherwise about-to-collide objects—was first noted by Schiehlen and Gao (Schiehlen 1987; Schiehlen and Gao 1989). Their one-dimensional (1D) model is essentially identical to the model we discuss here in more detail. Besides this one pair of papers, the literature on hopping and juggling does not seem to address the energy costs of finite-mass collisions or how to reduce their losses efficiently except by having light feet.

### 2.0.1. Hopping Research

The idea that the vertical motion in running might be something like a mass bouncing on a spring is intuitive enough. The coupling of this vertical motion to horizontal motion is slightly more subtle (see, for example, Alexander (1977)) but this was the basic scheme behind the successful powered robots of Raibert (see, for example, Raibert (1986)) studied analytically in, for example, Koditschek and Buehler (1991). In this class of model, the robot is a point mass or rigid body connected to the ground by a leg, containing a massless spring and actuator. The leg may or may not have rotary inertia, but this is irrelevant when only considering vertical hopping. The fully passive implementation of a related design was investigated in some detail by McGeer (1990). Ahmadi and Buehler (1997) have based a control scheme on stabilizing passive motions of this general type in order to save energy. But negative actuator work, rather than normal collisional energy loss, was the main issue because all of these models have no mass at the collision points (zero foot mass) and thus avoid the issue of collisional losses, at least for vertical hopping. Similarly, the control analysis of Francois and Samson (1994), as well as of Michalska, Ahmadi and Buehler (1996), is based on energy conserving motions where the foot has zero mass. The dead-beat controller in Canudas, Roussel, and Goswami (1997) neither uses fully passive motions as a base nor addresses energy efficiency issues. The possibility of wild dynamics of such controlled vertical hopping has also been studied (see, for example, M’Closkey, Vakakis, and Burdick (1990) and Vakakis and Burdick (1990)).

The issue of foot mass is considered explicitly in the elegant bow-leg design of Brown and Zeglin (Zeglin and Brown 1998; Brown and Zeglin 1998) which goes to pains to minimize the colliding mass, thus keeping energy loss from collisions as small as possible. They also surrender tight control of height and let the robot bounce passively for several bounces, until the peak height reaches a lower threshold, then injecting some energy at the next bounce. This approach seems to be simple, practical, and stable.

The hopping analysis of Berkemeier and Desai (2002) also ignores foot mass, but does address the trade-offs between simplicity of control design, stability, and actuator effort (although not energetic efficiency per se). They found, as did Schaal and Atkeson (1993) and Schaal, Sternad, and Atkeson (1996), that with an open-loop strategy where forcing is periodic with no feedback, stable hopping is possible. In these open-loop models, there are special conditions for periodic motions to be stable but the most efficient motions are on the boundary of this stability region. Thus, the open-loop motions are, if they are to be stable, inherently less than optimal in use of actuator effort.

The reality that the foot mass (sometimes called toe mass) is not zero is included explicitly in the hopping models of Rad, Gregorio, and Buehler (1993), Lapshin (1992) and Wei

et al. (2000), although none of the controllers discussed in these papers attempted to minimize the energy dissipated by collision (or, almost equivalently, from energy lost in active leg retraction).

### 2.1. One-dimensional Juggling Research

Closely related to hopping models are highly-simplified 1D juggling models where one object is repeatedly sent flying by a moving support. The first order of business is not keeping several balls aloft, as the word juggling might seem to imply, but keeping one ball in repeated stable vertical motion.

In extreme contrast to hopping models, which when simplified use zero foot mass, 1D juggling models are most often simplified by assuming infinite hand mass. That is, a hand is prescribed to move in a controlled manner that is unaffected by collisions with the juggled ball. Although the interaction of the ball with the hand is only intermittent and instantaneous in collisional juggling, Buehler, Koditschek, and Kindlmann (1994) found it fruitful to use active feedback of the hand throughout its motions, mirroring the ball's motion (times a factor) and then to correct based on a mismatch of actual and desired ball energy. Stable height control was found but actuator-effort issues were not addressed. Buehler and Koditschek (1990) have shown that, as for hopping models, with mistuning of the controller chaotic dynamics are possible.

Schaal and co-workers (Schaal and Atkeson 1993; Schaal et al. 1996; Sternad et al. 2000) have looked at an open-loop control of 1D impact juggling and have made several interesting observations. If a limit cycle is found for an oscillating hand (with perfect position control) then it is stable if the hand has a downwards acceleration at impact but not too strongly downwards, i.e., less in magnitude than

$$2g(1 + e^2)/(1 + e)^2, \quad (1)$$

where  $e$  is the coefficient of restitution. As noted by Berke-meier and Desai (2002), this finding seems to be related to their similar result for stability of an open-loop hopping robot. Sternad et al. (2000) noted that people who are given a racket and light ball seem to use this passive strategy. That is, to minimize effort people would presumably bounce a ball at the time of maximum vertical velocity of their vertically oscillating hand. Instead, they found that people prefer to hit the bouncing ball slightly *after* the peak velocity, during downward acceleration. Thus, it seems that people are willing to use some extra effort to improve the open-loop stability of the task. Not emphasized in the paper is that the cost in effort is often quite small; the phase shift from peak velocity to the impact people use leads to only a small reduction in impact velocity. That is, although the research does seem to show that people have a bias towards using open-loop (sensor-free) stability mechanisms in the juggling task, people use this mechanism with only a small cost in efficiency. A claim has been made, about which we have more to say in the discussion,

that dissipation is a necessary aspect of stability in open-loop systems.

Schaal and Atkeson (1993) have briefly discussed the little studied catch-and-release “Shannon” juggler (little studied, perhaps, because it works so well). The Shannon juggler uses  $e = 0$ , i.e., the ball is caught and does not bounce. Because the hand motion is prescribed, this is a deadbeat stabilizer; the ball is exactly returned to a fixed place in phase space after every catch. An interesting caveat, which we will discuss further, is that if the hand has a downward acceleration greater than  $g$  at the instant of contact, there is a bounce instead of a catch even though  $e = 0$ . A Shannon juggler with such  $e = 0$  bouncing does not have deadbeat stability and stability is instead ruled by the analysis given in, for example, Schaal et al. (1996).

Zavalo-Rio and Brogliato (1999) have considered the control of vertical juggling and, unlike in the other juggling papers above, have taken into account the hand mass and dynamics. They have found, according to the (untested by physical implementation) theory, robust stable controls more general than the “mirror” laws. They were not interested in energy efficiency issues.

### 2.2. Relevance of Existing Juggling and Hopping Literature

Besides the work of Schiehlen et al., all of the modeling research on hopping and juggling has at least one of the following three features: (1) massless collisions; (2) control; and (3) energy input. These three features are certainly reasonable in this era where just making a robot work well, however inefficient, is still an issue. There is no point in worrying about the fine points of efficiency and minimizing control effort for a robot that cannot do its job at all.

Looking ahead to an era where reducing actuator effort will be of more central concern, the work that follows has (1) massive collisions, and for most considerations, (2) no control and (3) no energy input. Instead, it is an investigation of simple passive means for avoiding collisional losses.

## 3. A Model for Passive Hopping

Our simple model is just two point masses connected by a linear massless spring (Figure 1). The subscript  $h$  for the masses denotes hopping (as opposed to  $j$  for juggling). These represent, roughly, a body connected elastically to non-massless feet. There is no control and no energy input. The only dissipation occurs when the lower mass strikes the ground. Except where explicitly stated in the discussion, we assume plastic impact with a coefficient of restitution  $e = 0$ , i.e., the velocity of  $m_{2h}$  becomes zero on impact. The relaxed spring length  $L_o$  is large enough to keep the masses separated at all times.

The motion has two continuous phases: (1) flight when both masses are in the air; and (2) contact, when  $m_{2h}$  is in steady contact with the ground. There are two transitions: (3) impact (collision, landing), when the velocity of  $m_{2h}$  jumps

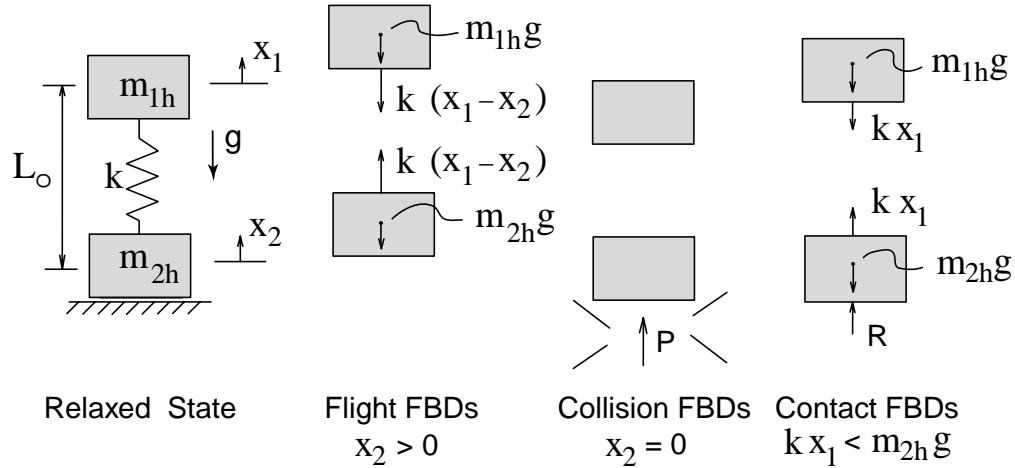


Fig. 1. The hopping “h” model: two point masses connected by a massless spring. The “foot”  $m_{2h}$  has plastic collisions with the ground.  $x_i$  are zero when  $m_{2h}$  is on the ground and the spring has no tension. The free body diagrams (FBDs) for the pairs of masses are shown for all three cases where momentum balance is used: flight, collision, and contact. The dimensionless equations used in the text correspond to  $m_{1h} = 1$ ,  $m_{2h} = M_h \equiv M$ ,  $k = 1$ , and  $g = 1$ .

to zero; and (4) lift-off, when  $m_{2h}$  is lifted from contact into flight.

### 4. Equations of Motion for Hopping

**Flight.** The non-dimensional equations of motion for flight are (see Figure 1):

$$\begin{aligned} (1 + M_h)\ddot{y}_1 &= -M_h(y_1 - y_2) - 1 \\ (1 + M_h)\ddot{y}_2 &= (y_1 - y_2) - 1. \end{aligned} \tag{2}$$

Here  $y_1 = x_1/(m_{2h}g/k)$ ,  $y_2 = x_2/(m_{2h}g/k)$ ,  $M_h = m_{2h}/m_{1h}$ , and  $(\dot{\phantom{y}}) \equiv d(\phantom{y})/d\tau_h$  where  $\tau_h = \omega_h t$  with  $\omega_h = \sqrt{k(1 + M_h)/m_{2h}}$  being the angular frequency of vibration in the flight phase. The dimensionless equations have only one parameter,  $M_h$ . The dimensionless equations correspond to  $m_{1h} = 1$ ,  $m_{2h} = M_h$ ,  $k = 1$ , and  $g = 1$  in Figure 1.

**Collision Transition.** The collision causes a jump in velocities but not in displacements. Using “-/+” to denote before and after impact, the collision occurs when  $y_2^- = 0$  and  $\dot{y}_2^- \leq 0$ . The impact transitions are  $y_1^+ = y_1^-$ ,  $y_2^+ = y_2^- = 0$ ,  $\dot{y}_1^+ = \dot{y}_1^-$ , and  $\dot{y}_2^+ = 0$ .

**Contact.** During a period of sustained contact,  $y_2 \equiv 0$ ,  $y_1 < 1$  and  $(1 + M_h)\ddot{y}_1 = -M_h y_1 - 1$ .

**Lift-off Transition.** Lift-off from contact occurs when the spring tension lifts the lower mass and  $y_1 = 1$ . The lift-off condition can also be met immediately at contact with no period of sustained contact (if  $y_1^- > 1$ ). At lift-off from sustained contact, there is no jump in position or velocity of either mass.

We define  $\alpha \equiv \dot{y}_1$  at lift-off after a period of sustained contact.  $\alpha$  is the key variable in the following analysis. The positions and velocities at lift-off are

$$y_1 = 1; \quad \dot{y}_1 = \alpha; \quad y_2 = 0; \quad \dot{y}_2 = 0. \tag{3}$$

These serve as initial conditions for the flight equations. Note that all subsequent motions for all time are determined by  $\alpha$  at one lift-off. Thus, the dynamics can be characterized by a 1D map,  $\alpha_{n+1} = f(\alpha_n)$ . One-dimensional maps have been used to study hopping in the past (see, for example, Koditschek and Buehler (1991)), but not for passive hoppers.

### 5. A Model for Passive Juggling

The juggling model is shown in Figure 2. It consists of a free point mass  $m_{1j}$ , and a point mass  $m_{2j}$  connected to the ground by a massless, linear spring of stiffness  $k$ . The model is passive and the collisions between the masses are assumed to be plastic. The masses are assumed to have vertical motion only. This is like a single mass bouncing with no restitution on a trampoline with mass (a second mass supported by a spring). Alternatively, this is also a model of juggling with the support being a passive oscillator.

As in the hopping model, the juggling model has four phases: two continuous phases, (1) flight phase, with  $m_{1j}$  moving under gravity and  $m_{2j}$  having oscillatory motion; (2) contact phase, where  $m_{1j}$  is in steady contact with  $m_{2j}$ ; and two transition phases, (3) impact between the masses; and (4) lift-off, where there is a loss of contact between the two masses.

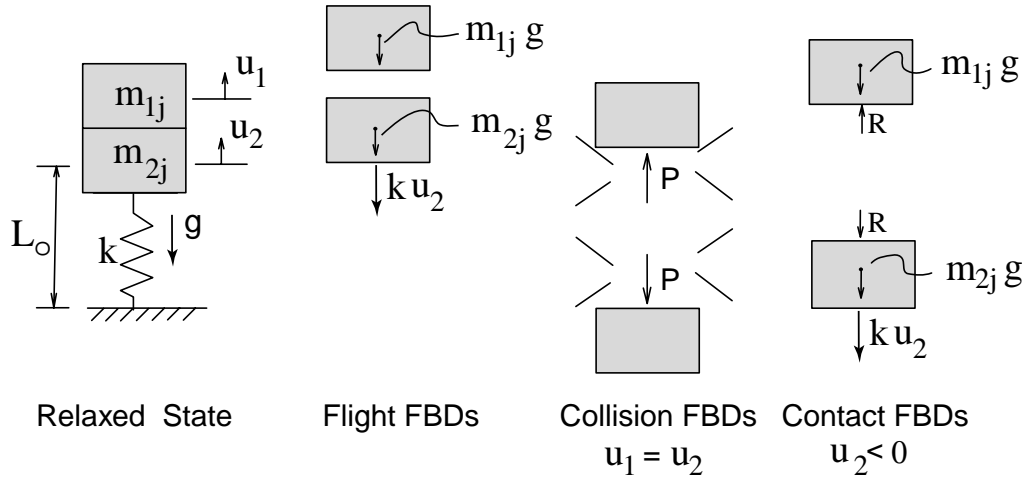


Fig. 2. The juggling “j” model: two point masses representing a ball  $m_{1j}$  and a hand  $m_{2j}$ .  $m_{1j}$  is free and  $m_{2j}$  is connected to the ground by a massless spring.  $u_i$  are zero when the spring has no tension and the masses are in contact. The masses have plastic collisions with each other. Free body diagrams (FBDs) are shown for each of the phases where momentum balance is used for equations of motion: free flight, collision, and sustained contact. The dimensionless equations in the text correspond to  $m_{1j} = 1$ ,  $m_{2j} = M_j \equiv M$ ,  $k = 1$ , and  $g = 1$ .

## 6. Equations of Motion for Juggling

**Flight.** The non-dimensional equations of motion for flight are: (Figure 2)

$$\begin{aligned}\ddot{w}_1 &= -1 \\ \ddot{w}_2 &= -w_2 - 1.\end{aligned}\quad (4)$$

Here  $w_1 = u_1/(m_{2j}g/k)$ ,  $w_2 = u_2/(m_{2j}g/k)$ , and  $(\dot{\phantom{x}}) \equiv d(\phantom{x})/d\tau_j$  where  $\tau_j = \omega_j t$  with  $\omega_j = \sqrt{k/m_{2j}}$  being the frequency of vibration of  $m_{2j}$ . The dimensionless equations correspond to  $m_{1j} = 1$ ,  $m_{2j} = M_j$ ,  $k = 1$ , and  $g = 1$  in Figure 2.

**Collision Transition.** The collision occurs when  $w_1 = w_2$  and  $\dot{w}_1 < \dot{w}_2$ . Immediately after the collision,  $m_{1j}$  and  $m_{2j}$  have the same speed. Using “-/+” to denote before and after impact, we have  $w_1^+ = w_1^- = w_2^+ = w_2^-$ . Also  $\dot{w}_1^+ = \dot{w}_2^+$ . Using the balance of linear momentum, the speed of both the masses just after the impact is given as

$$\dot{w}_1^+ = \dot{w}_2^+ = \frac{\dot{w}_1^- + M_j \dot{w}_2^-}{1 + M_j},$$

where  $M_j = m_{2j}/m_{1j}$ .

**Contact.** During a period of sustained contact between  $m_{1j}$  and  $m_{2j}$ , we have  $w_1 = w_2 < 0$ . There is oscillatory motion with both masses moving as one. This oscillatory motion is given as

$$(1 + M_j)\ddot{w}_2 = -M_j w_2 - (1 + M_j).\quad (5)$$

**Lift-off Transition.** There is a loss of contact between the two masses after a period of sustained contact when the acceleration of the masses is  $-g$ . Equivalently, in non-dimensional quantities this condition is met when  $\ddot{w}_1 = \ddot{w}_2 = -1$  or when  $w_1 = w_2 = 0$ . There can be a loss of contact immediately after impact if  $w_1^+ = w_2^+ > 0$ .

## 7. Equivalence of Hopping and Juggling Equations

The hopping model has identical dynamics to the juggling model. The flight and contact equations for the hopping model reduce to the flight and the contact equations for the juggling model by this change of variables and system parameters

$$\begin{aligned}w_1 &= (y_1 - 1) + M_h y_2 \\ w_2 &= (y_1 - 1) - y_2 \\ M_j &= M_h \quad (\text{henceforth called just } M)\end{aligned}\quad (6)$$

with a scaling of the two dimensionless times  $\tau_j = \sqrt{M/(1+M)} \tau_h$ .

In the hopping model during the collision transition, we have  $\dot{y}_2^+ = 0$  and  $\dot{y}_1^- = \dot{y}_1^+$ . In the juggling model, just after the impact, the speed of both masses is  $\dot{w}_1^+ = \dot{w}_2^+ = (\dot{w}_1^- + M\dot{w}_2^-)/(1+M)$ . Using the equivalence relations in eq. (6), we have

$$\dot{w}_1^+ = \dot{w}_2^+ = \dot{y}_1^+.$$

The equivalence relations in eq. (6) also show that the conditions for lift-off in the hopping model after a period of sustained contact, i.e.,  $y_1 = 1$  and  $y_2 = 0$ , correspond to  $w_1 = w_2 = 0$ , which are the conditions for loss of contact (after a period of sustained contact) in the juggling model. Also, eqs. (6) show that the conditions for immediate lift-off after impact in the hopping model, i.e.,  $y_1^+ > 1$  and  $y_2^+ = 0$ , correspond to  $w_1^+ = w_2^+ > 0$ , which is the condition for a loss of contact immediately after impact in the juggling model.

Because of the equivalence of the two systems, we can use either one for discussion.

**Nature of Solutions in General.** Here we describe motions in the hopping model, not yet looking for impact-free solutions. A solution results from pasting together the flight, contact and collisional phases. In flight, the center of mass moves as a particle thrown vertically in a gravitation field. The masses oscillate sinusoidally around this mean parabolic motion. At collision,  $m_{2h}$  stops dead and the upper mass is unperturbed. If sustained contact follows,  $m_{2h}$  is stationary and  $m_{1h}$  has simple harmonic motion until the next lift-off when the spring tension matches  $m_{2h}g$ .

In the juggling model the flight phase consists of the upper mass in a parabolic (height versus time) free fall while the lower mass oscillates sinusoidally on its support spring. On impact, the two velocities instantaneously become equal, while also conserving momentum. If sustained contact follows, the two masses oscillate together as supported by the spring until lift-off when the downwards acceleration of the pair reaches  $-g$ .

## 8. Lossless Collisions

Lossless motions for the hopper can occur only if  $m_{2h}$  impacts the ground with zero speed (see Figure 3). Refer to Figure 4 to see how lossless motion is special. In Figure 4(a) the impact has non-zero speed and would be dissipative. Thus, for no dissipation,  $\dot{y}_2 = 0$  at  $y_2 = 0$ . In Figure 4(b) the impact occurs at zero speed. But because  $\ddot{y}_2 > 0$ , contact would be immediately lost and there would be a subsequent collision with non-zero speed, so we need  $\ddot{y}_2 \leq 0$ . Figure 4(c) shows an impact at zero speed, but with prior ground penetration because  $\ddot{y}_2 < 0$ , so we need  $\ddot{y}_2 \geq 0$ . Thus, for lossless impact at  $y_2 = 0$ , not only  $\dot{y}_2 = 0$ , but also  $\ddot{y}_2 = 0$ . Because  $\ddot{y}_2 = 0$ , the ground clearance condition is determined by  $d^3y_2/d\tau^3$ . Figure 4(d) shows a conceivable collision with  $y_2 = 0$ ,  $\dot{y}_2 = 0$ ,  $\ddot{y}_2 = 0$  but with  $d^3y_2/d\tau^3 > 0$ . This is disallowed because this grazing would be followed by a dissipative impact.

Thus we must simultaneously meet all of these conditions at the end of flight

$$y_2 = 0, \quad \dot{y}_2 = 0, \quad \ddot{y}_2 = 0 \quad \text{and} \quad d^3y_2/d\tau^3 < 0$$

as shown in Figure 4(e). Somewhat remarkably perhaps, all of these conditions can be simultaneously met in this model, no

matter what the values of the model parameters, by adjustment of the single dynamic variable  $\alpha$  (the lift-off speed of  $m_{1h}$ ).

To find these lossless solutions, we first solve the initial value problem for the flight phase (eqs. (2) and (3)). By elementary methods, the solution is

$$(1 + M)y_2 = 1 + \alpha\tau - \frac{\tau^2}{2} - \alpha \sin \tau - \cos \tau, \quad (7)$$

$$(1 + M)y_1 = 1 + \alpha\tau - \frac{\tau^2}{2} + M(\alpha \sin \tau + \cos \tau). \quad (8)$$

Let the time of flight be  $\tau_f$ . Imposing dissipation-free contact, we have

$$y_2(\tau_f) = 0; \quad \dot{y}_2(\tau_f) = 0; \quad \ddot{y}_2(\tau_f) = 0 \quad (9)$$

and the inequality condition  $d^3y_2(\tau_f)/d\tau^3 < 0$ . Equations (9) are three equations in two variables,  $\tau_f$  and  $\alpha$  ( $M$  is fixed). At first sight, the system appears over-determined. Nonetheless, solutions do exist. From eqs. (7) and (9) we obtain

$$1 + \alpha\tau_f - \frac{\tau_f^2}{2} - \alpha \sin \tau_f - \cos \tau_f = 0 \quad (10a)$$

$$\alpha - \tau_f - \alpha \cos \tau_f + \sin \tau_f = 0 \quad (10b)$$

$$-1 + \alpha \sin \tau_f + \cos \tau_f = 0. \quad (10c)$$

Substituting eq. (10c) into eq. (10a) we obtain  $\alpha\tau_f - \frac{\tau_f^2}{2} = 0$ , which implies

$$\tau_f = 2\alpha \quad (11)$$

(since  $\tau_f \neq 0$ ). Substituting eq. (11) into (10c), we obtain

$$\alpha = \tan \alpha. \quad (12)$$

Satisfaction of eqs. (11) and (12) forces satisfaction of eq. (10b) in addition to eqs. (10a) and (10c), as well as the inequality condition  $d^3y_2(\tau_f)/d\tau^3 < 0$ . Equation (12) has infinitely many solutions for  $\alpha$  (and hence for  $\tau_f$ ). These solutions for  $\alpha$  which give incessant hopping are denoted by  $\alpha^*$  and equal 4.493409, 7.725251, 10.90412, ... . Higher values of  $\alpha^*$  correspond to more oscillations between collisions. For the first root,  $\alpha^* = 4.4934$ ; the solution is shown in Figure 3 (using  $M=1$ ). We have also independently verified the observed persistent motion using a commercial dynamic simulation package (Working Model), where, to our initial surprise, the motion appeared stable (more about this later).

Summarizing, for values of  $\alpha^*$  that satisfy  $\alpha = \tan \alpha$ , the initial conditions given in eq. (3) lead to incessant hopping solutions. In terms of dimensional quantities, for incessant hopping,

$$\left. \frac{dx_1}{dt} \right|_{t=0} = \alpha^* g \sqrt{\frac{M(m_{1h} + m_{2h})}{k}}. \quad (13)$$

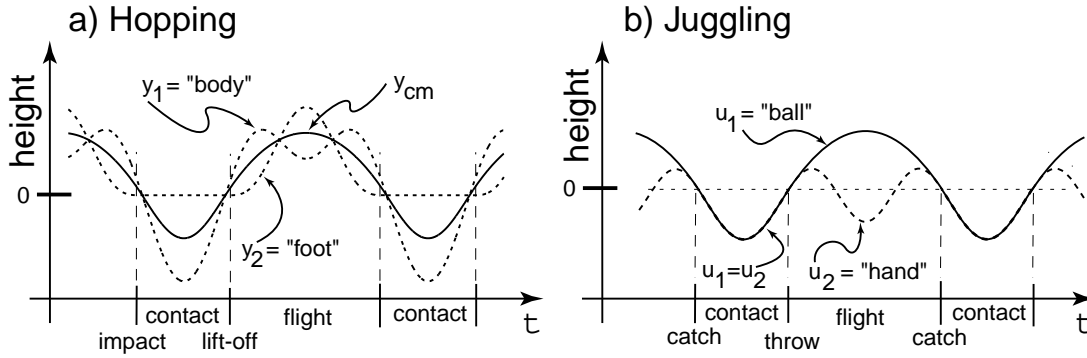


Fig. 3. (a) A lossless periodic motion of the hopper showing foot, body, and center-of-mass trajectories. (b) Lossless periodic motion of the juggler showing ball and hand trajectories. The ball trajectory of the juggler matches the center-of-mass trajectory of the hopper if the masses are appropriate, as in the figure where  $M = 1$  in both cases.

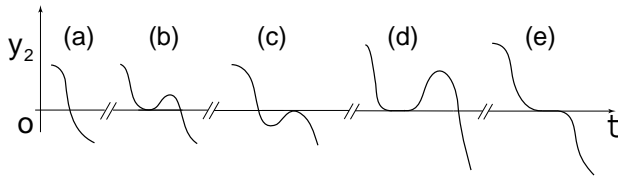


Fig. 4. Different conceivable motions of  $m_{2h}$  near impact, but showing ground penetration (see text).

Equation 13 shows that for any hopper of fixed total mass and fixed  $k$ , as the mass ratio  $M$  becomes smaller (i.e., as the foot mass becomes lighter and lighter compared to the torso), the incessant hopping solutions  $(dx_1/dt)|_{t=0}$ , corresponding to the various  $\alpha^*$  values, become closer and closer. Approaching the singular limit,  $M \rightarrow 0$ , every  $(dx_1/dt)|_{t=0}$  becomes arbitrarily close to an incessant hopping solution  $\alpha^*$ . In this way, the limiting behavior of the model agrees with the behavior of the model in the limit.

Because of the equivalence of the hopper and juggler we need not repeat the arguments above for the juggling model. The same values of  $\alpha^*$  correspond to the vertical velocities of the hand and ball at separation for solutions where the subsequent collision is at zero relative velocity. Also, as the singular limit  $M \rightarrow 0$  (massless hand) is approached, all (large enough) hand velocities become arbitrarily close to some incessant juggling solution.

## 9. Analysis Through 1D Maps

We investigate the dynamics of the model for general solutions using a numerically constructed map,  $\alpha_{n+1} = f(\alpha_n)$ . The map counter  $n$  is only incremented after sustained contacts (if the

map counter were incremented after non-sustained contacts we could not reduce the system to a 1D map). We find  $f$  by inserting  $\alpha_n$  as a parameter in eq. (10a) and solving for  $\tau_f$ . If  $y_1 \geq 1$  at impact there is immediate lift-off. If so, we solve the flight equations forward until the next contact. If  $y_1 < 1$ , there is sustained contact and  $\alpha_{n+1}$  is found from the post-impact state using energy balance. The 1D map for  $M = 1$  is shown in Figures 5(a) and (b). The graph remains below the line  $\alpha_{n+1} = \alpha_n$  as non-negative energy dissipation demands.

Just to the right of the  $\alpha^*$  points, there are no bounces between sustained contacts. Just to the left of  $\alpha^*$  there is one non-sustained-contact bounce between sustained contacts, hence the discontinuity in the slope of the map.

**The Case of  $M \rightarrow 0$ .** As expected, the numerics show that, for  $M \rightarrow 0$ , the  $\dot{y}_1$  values corresponding to  $\alpha^*$  bunch up, and values of the 1D map approach the identity line between  $\alpha^*$  values as well (see Figure 5(c)), as one would expect from the spring-mass hopping model with negligible unsprung mass or from a juggling model with a nearly massless hand.

**The Case of  $M \rightarrow \infty$ .** Somewhat similarly, as  $M \rightarrow \infty$  the map approaches the identity line except for in some narrow but non-vanishing regions (Figure 5(d) shows one of these regions). We describe this situation using the juggling model (for the hopping model with  $M \rightarrow \infty$ ,  $y_1 \rightarrow \infty$  at the  $\alpha^*$  solutions which impedes simple discussion). If the hand mass is much larger than the ball mass, one expects that one collision would little affect the next throw; thus, two successive throws should be close and the map should be close to the identity line as is observed for most of the map. However, in the narrow region where the map deviates significantly from the identity line, there are many bouncing (non-sustained contact) impacts between map evaluations and their cumulative effect is significant. As  $M \rightarrow \infty$ , the number of these impacts apparently also goes to  $\infty$ , as suggested by numerics and as can also be informally reasoned as follows.

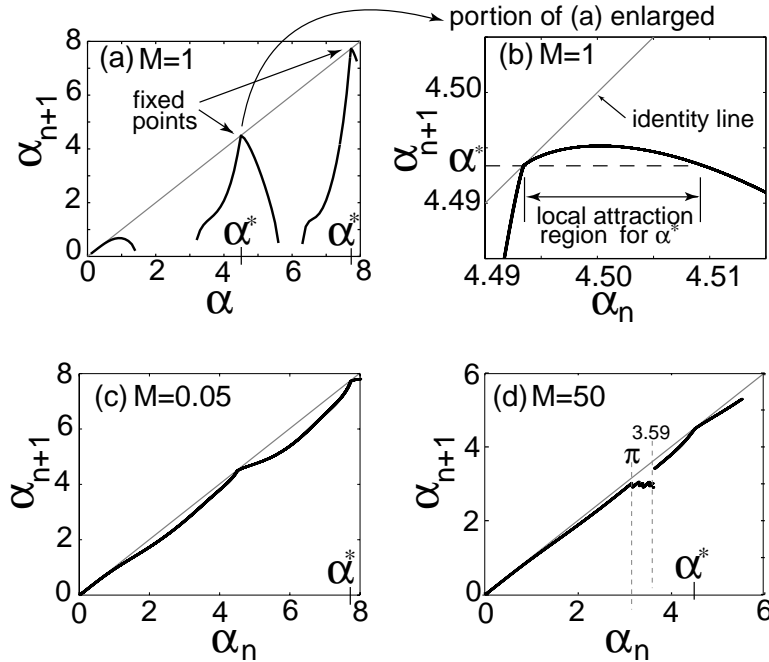


Fig. 5. The 1D map for the hopping model with  $M = 1$ . An enlarged portion of (a) is shown in (b) (enlarged about 300 times). The fixed point  $\alpha^*$  has one-way stability. (c) shows that the map is close to the identity line for a low value of  $M$ . (d) shows that for a large value of  $M$  the map is close to the identity line but for a small neighborhood bounded below by  $\pi$  and above by about 3.59.

In the limit  $M = \infty$ , the juggling hand has unperturbable sinusoidal oscillations. The bouncing analysis of Schaal et al. (1996) applies for  $e = 0$  if there is no sustained contact (only bouncing). Applying the condition that there be periodic motions ( $\dot{w}_1 = \pi$  at impact), that there be no sustained contact ( $\ddot{w}_1 < -1$ ), and that the periodic motions be stable ( $\dot{w}_1 > -2$ , from eq. (1) with  $e = 0$ ), for the sinusoidal motion of the hand we find a range of amplitudes for which there can be stable bouncing in the model of Schaal et al. (1996).

For oscillations of the lower mass at any amplitude within this range of stable bouncing, there is also a time when the condition for a throw after a sustained contact is met (i.e., where the downwards acceleration of the lower mass is  $-1$ ). In evaluating our map numerically, we assume that the upper mass is thrown at that same point; the speed  $\dot{w}_1$  with which the upper mass is thrown depends on the amplitude of the lower mass oscillation. The throwing speeds, when the motion is such that stable bouncing is possible, are in the range:

$$\pi < \dot{w}_1 < \sqrt{\pi^2 + 3} \quad \text{or approximately} \quad 3.14 < \dot{w}_1 < 3.59.$$

Subsequent motion after a throw at a speed in this range, since the period-one bouncing–juggling solution is asymptotically stable, should converge to that period-one bouncing solution. Thus, after a throw (and map evaluation) motion converging to stable bouncing continues indefinitely, there is no more

sustained contact, and the map cannot be evaluated again. At least, for  $M \equiv \infty$ .

If  $M$  is very large but finite, we expect the time history of the motion to look approximately like the infinite  $M$  solution above, except that the amplitude of oscillation of the lower hand mass now slowly decreases as the upper mass continues bouncing on it and slowing it, again and again. This process continues until the amplitude of the hand motion is not large enough to support stable bouncing  $\dot{w}_1 < \pi$ . The bouncing solutions then give way to a solution including a sustained contact, and the map is finally evaluated.

At the high amplitude end of the stable bouncing region things are slightly less clear. Where the analysis of Schaal et al. (1996) predicts a loss of linearized stability, a small window of stable period-two bouncing solutions seems (in our numerics) to be stable. So the right boundary of the triangular region of the map protruding from the identity line goes slightly past the upper limit of stable period-one bouncing solutions at  $\sqrt{\pi^2 + 3}$  because throws in this range also lead to stable period-two bounces that continue until the period-one bounces take over and the energy of the massive hand is attenuated.

So, for any large but finite  $M$  we expect a map similar to Figure 5(d) where in the funny level (triangular jog) region a single map evaluation (from one throw after sustained contact

to the next) is evaluated with a series of bouncing contacts between.

**One-sided Stability.** The fixed points of the map are the non-dissipative solutions discussed previously. As for any map with a hump tangent to the identity line (see, for example, Figure 2 in Goldhirsch, Noskowitz, and Schuss (1993) and references therein), a so-called “tangent bifurcation” that typically occurs at special parameter values for many systems, the fixed points have one-sided stability. Figure 5(b) shows that the map, in the neighborhood of each fixed point, locally has two distinct behaviors: to the left of the fixed point, the map has a slope greater than one, while to the right it is tangent to the identity line at  $\alpha^*$ .

Any trajectory starting from an initial condition just to the right of  $\alpha^*$  will eventually go to the fixed point. However, an initial condition just to the left will diverge and could be attracted to a solution at a smaller  $\alpha^*$ . As a consequence, the basin of attraction for any fixed point  $\alpha^*$  can be quite complex, as discussed in some detail by Reddy and Pratap (2002).

By most definitions of stability, the persistent solutions are unstable; there are infinitesimal perturbations (to the left of the tangent point) which grow as the map is iterated. However, the one-sided stability is perhaps less unstable than the technically applicable description “unstable” would imply, in that there is a set of initial conditions with finite (non-zero) measure that become attracted to the periodic motions. In other words, one does not need infinite precision to locate a point on the attracting set.

As mentioned above, such one-sided stability is a commonly observed feature of systems undergoing “tangent” bifurcations. Note, however, that (unless imbedded in a more complex model) our system is not at a bifurcation point; the tangency persists for all values of free system parameters in this otherwise-conservative system with dissipative collisions.

**Symmetry of Special Solutions.** Figure 6(a) shows a typical non-incessant trajectory of  $m_{2h}$ , implicitly including impact impulse  $P$ . Played backwards, this motion would be a solution only if, at lift-off, an impulse  $P$  acted from the ground. Since the model does not allow a lift-off impulse, a typical motion is not time reversible.

Now we consider an incessant hopping solution (Figure 6(b)). Having no landing impulse, it may be reversible in time for a full motion cycle (flight, contact, lift-off and landing). Using eqs. (10c) and (12) in (8), we see  $y_1(\tau_f) = 1 = y_1(0)$ . Similarly from eqs. (8) and (10b),  $\dot{y}_1(\tau_f) = -\alpha^*$ .

A time-reversed incessant trajectory, being a valid solution, satisfies the lift-off condition  $y_1 = 1$ . By energy conservation, the system energy (KE+PE) at lift-off and landing are the same. Thus, the incessant hopping solution has landing with  $y_1 = 1$  and  $|\dot{y}_1| = \alpha$ . Now  $\dot{y}_1 = +\alpha$  at landing is impossible because lift-off occurred at  $\dot{y}_1 = \alpha$ , and (because of gravity) the momentum of the system is not conserved during

flight ( $\dot{y}_1 = +\alpha$  would incorrectly conserve momentum). So  $\dot{y}_1 = -\alpha$ . Thus, for the incessant motions, a time-reversed solution is not only a solution (as for all classical non-dissipative mechanical systems) but also the same solution (the movie played backwards is the same movie).

### Persistent Hopping Does Not Depend on Spring Linearity.

The above symmetry discussion used the time-reversal invariance of the equations but neither spring linearity nor gravity constancy. So even for hoppers with non-linear springs in a non-uniform gravitational field, if there are any incessant hopping solutions, they must have time-reversal symmetry.

Here is a qualitative consistency argument for the existence of incessant hopping with a non-linear spring and varying-with-height gravity. Consider motions that at some reference time in the flight have center-of-mass height  $h$ , compression  $a$  of the spring and  $\dot{y}_1 = \dot{y}_2 = 0$ . These conditions generate a time-symmetric trajectory with the reference time being mid-flight. Now look at a family of such motions where  $h$  is fixed and  $a$  is varied (Figure 7). For small enough  $a$ , the trajectory of  $m_{2h}$  has no extrema after mid-flight. For large enough  $a$ , the trajectory of  $m_{2h}$  has one or more pairs of extrema. For an intermediate value of  $a$ , two extrema merge and two of the dissipation-free impact conditions are met ( $\dot{y}_2 = 0$  and  $\ddot{y}_2 = 0$ ). Now adjust  $h$  to achieve the condition  $y_2 = 0$  (while continuously adjusting  $a$ , if necessary, to maintain the inflection condition).

The solution thus obtained is a persistent hopping solution. That is, persistent hopping solutions are expected even for the energy-conserving model perturbations of a non-uniform gravitational field and/or non-linear springs (assuming the non-linearities do not disrupt center-of-mass flight time increasing monotonically with  $h$  and the oscillatory nature of the motions relative to the center of mass in flight).

**Viscous Damping Destroys Incessant Hopping.** Under dissipative perturbations (damping), the map shifts generally downwards, loses contact with the identity line, and incessant hopping is lost as shown schematically in curve (a) of Figure 8.

### Small Energy Injection Stabilizes Persistent Hopping.

With small energy input, such as by incrementing  $\alpha$  by a small amount  $\epsilon$  at every step, the map will move generally up, as in curve (c) of Figure 8, drawn for the case  $M = 1$ . The map will then cut the identity line at two fixed points: one stable and the other unstable. Thus, we can obtain incessant motion with bidirectional stability by injecting a small amount of energy at each hop. To correspond with exactly displacing the curve upwards, one would add a fixed increment in launch velocity, but the qualitative result does not depend on any precise form of energy injection. Presumably, small numerical errors equivalent to energy inputs caused the apparent stability of motions in the Working Model numerical simulation mentioned in Section 8.

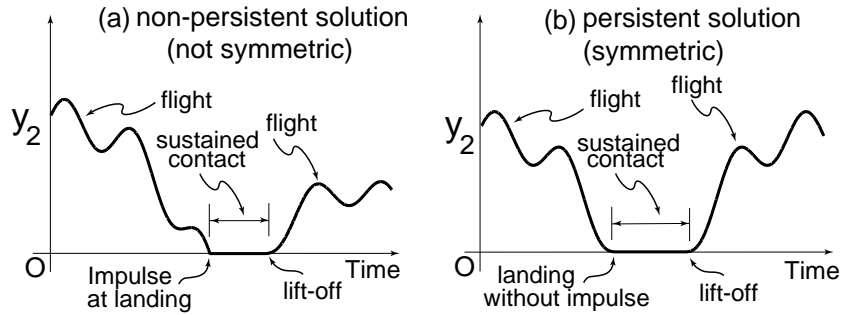


Fig. 6. A typical trajectory of the lower mass of the hopper with (a) an impulse at landing and (b) no impulse at landing.

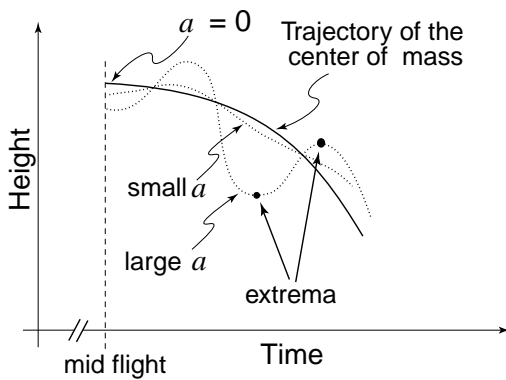


Fig. 7. Effect of the compression  $a$  of the spring at the instant of maximum height on the trajectory of the lower mass.

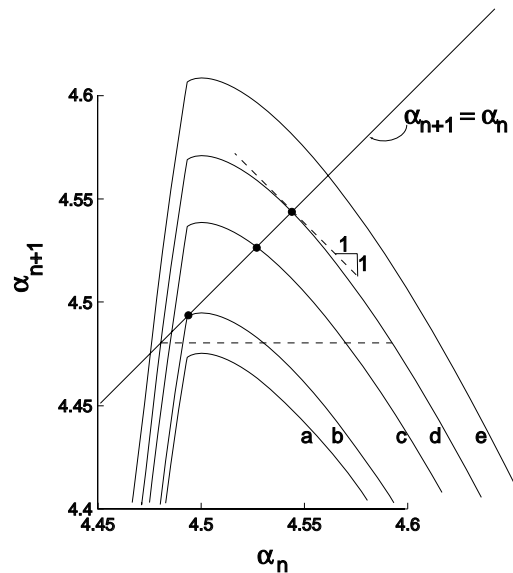


Fig. 8. The map near the first nominal fixed point when energy is added or subtracted for  $M = 1$ . Curve (b) is the basic system of study with the semi-stable fixed point marked with a dot. If energy is removed at every hop, more exactly if the launch velocity is diminished by a fixed constant, the curve is displaced down as in (a). There is no fixed point. If the curve is moved up by the injection of energy as in curve (c) the upper intersection of the map with the identity line, marked with a dot, becomes stable. Curve (d) is the map with the greatest injection of energy for which the upper fixed point is stable. This curve also maximizes the basin of attraction shown by the horizontal dotted line. As the map is lifted through this configuration there might be a period doubling bifurcation (not investigated). If the map is displaced above (d) there is no stable fixed point, as in curve (e) although some non-periodic orbit could still be attractive.

For values of  $M$  not far from 1, the global basin of attraction of a stable fixed point is actually quite complex, due to humps in the map from greater values of  $\alpha^*$ . However, for simplicity, we briefly examine the local basin of attraction, meaning that part of the basin which is an open interval containing the  $\alpha^*$  of interest. The size of this basin is one measure of stability.

Without energy injection, the size of the local basin is zero (the finite-sized one side gets no credit because the motion is unstable). For infinitesimal energy injection, there is a small basin whose size grows with the amount of energy injected. As the amount of energy injected increases further, the hitherto stable fixed point eventually loses stability when the map has a slope of  $-1$  at the upper fixed point, possibly through a period doubling bifurcation (as in M'Closkey et al. (1990) and Vakakis and Burdick (1990)). At this point, for the  $M = 1$  case shown, the local basin will have maximal size (as shown in Figure 8 by a horizontal dashed line). When the map is lifted above this point, as in curve (e) of Figure 8, the period-one motion loses stability.

## 10. Physical Demonstrations

As a physical test of the model and to set the ideas out clearly, we set up a table-top demonstration experiment. This does nothing, of course, to show the utility of the present concepts in a practical robot. We set up the juggling version of the model using a standard freshman-physics demonstration air track with two available masses and tension springs. The track was tipped with a block to simulate reduced gravity (see Figure 9).

In this experiment, the maximum-compression release-from-rest position was tuned, by trial and error, to find the motion where the catching collision was as gentle as possible and with only one oscillation of the hand (left,  $m_2$ ) mass during flight. No theoretical calculations were made for the predicted amplitudes before the measurements. The amplitudes of motion of both  $m_1$  and  $m_2$  were measured for these motions. These amplitudes and their ratios were then compared with the model-predicted values as follows.

Let  $A_1 = h + h_2$  and  $A_2 = h_1 + h_2$  (see Figure 10) be the amplitudes of motion of  $m_1$  and  $m_2$ , respectively. We can determine  $h$ ,  $h_1$  and  $h_2$  from eqs. (4) and (5). Since these equations apply between collisions, we can use conservation of energy to find

$$\begin{aligned} h &= \frac{\dot{w}_1^2}{2} \\ h_1 &= -1 + \sqrt{1 + \dot{w}_1^2} \\ h_2 &= \frac{1 + M}{M} \left[ 1 + \sqrt{1 + \frac{M}{1 + M} \dot{w}_2^2} \right]. \end{aligned} \quad (14)$$

Note that  $h_2$  is obtained from the contact equation in which we can use either  $\dot{w}_1$  or  $\dot{w}_2$  since  $\dot{w}_1 = \dot{w}_2$ . Using  $M = 0.909$  (from  $m_1 = .2923$  kg and  $m_2 = .2657$  kg) and  $\dot{w}_1 = \dot{w}_2 = \alpha^* = 4.4934$ , we obtain  $h = 10.095$ ,  $h_1 = 3.603$ ,  $h_2 = 8.942$ , so that the model predicts dimensionless  $A_1 = 19.037$  and  $A_2 = 12.545$ . Note that the amplitude ratio  $A_1/A_2$  (like any ratio of sums or differences of any of  $h_1$ ,  $h_2$  or  $h$ ) is independent of the dimensional scaling (and thus independent of  $g$ ). Thus we have

$$\begin{aligned} (A_1/A_2)_{model} &= 1.517 \pm 3\% \quad \text{and} \\ (A_1/A_2)_{exp} &= 1.523 \pm 3\%. \end{aligned}$$

The 0.4% difference between theory and experiment is far within the estimated cumulative error bound of 6%.

To compare the experimental values of the absolute dimensional amplitudes with the corresponding predicted values, we need to dimensionalize the predicted  $A_1$  and  $A_2$ . We find the dimensional amplitudes by multiplying with the scaling factor  $m_{2j}g/k$  (recall that  $w_1 = u_1/(m_{2j}g/k)$  and  $w_2 = u_2/(m_{2j}g/k)$ ). The gravity constant  $g$  in the model corresponds to the effective air-track gravity of  $g \sin \theta$ . The air track was tipped up by 1.1 inch over a five foot horizontal distance. Thus, the slope  $\theta = \tan^{-1}(1.1/60) = 1.83 \times 10^{-2}$ . The

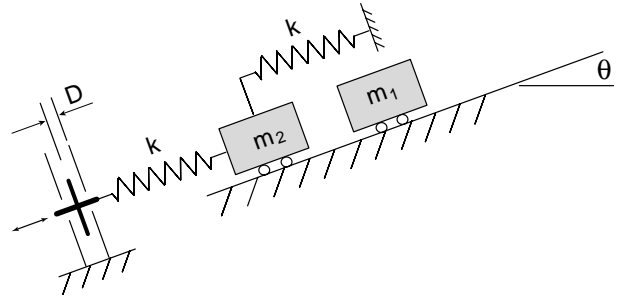


Fig. 9. Schematic diagram of the air-track juggling experiment. A freshman-physics style air track was propped with a book to an angle of about  $1^\circ$ .  $m_1 = 292.3$ g,  $m_2 = 265.7$ g. To avoid compression in the springs, two springs were pre-stretched end-to-end as shown, with  $k_{net} = 2k = 8.8$  N m $^{-1}$ . The normally elastic bumpers were padded with paper to deaden the collisions. Motion is initiated by holding  $m_1$  to the left of equilibrium, with  $m_2$  resting against it, and then releasing it. The minimum displacement that leads to a smooth recapture is the primary experiment. Secondly, an attempt to sustain oscillations was made by adding a small amount of energy during each cycle by moving the spring end back and forth a distance  $D = 3$ mm; to the right when  $m_2$  is at its left extreme and to the left when  $m_2$  is at its right extreme. Up to eight sequential smooth collisions could be obtained.

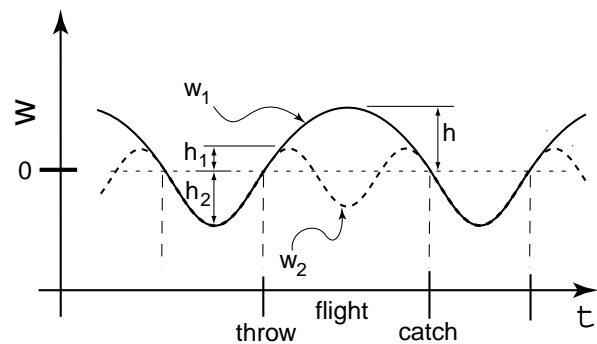


Fig. 10. The amplitudes of oscillation of the two masses in the juggling model are shown to indicate measurements made in the juggling experiment.

spring stiffness was measured independently by timing the oscillations of a known hung mass. The scaling factor is thus computed to be  $m_{2j}g \sin \theta / k = 5.431 \times 10^{-3} \text{m}$ . Therefore,

$$(\Delta u_1)_{model} = 0.103\text{m} \pm 9\% \quad \text{and}$$

$$(\Delta u_1)_{exp} = 0.099\text{m} \pm 1\%.$$

The 4% difference between theory and experiment is well within the estimated cumulative error bound of 10%.

Up to eight smooth collisions, and then only rarely, could be obtained with hand forcing. Not more, presumably because the accuracy of the energy stimulus was not good enough for the small domain of attraction of the periodic motions. Note, however, that the experiment is close to the  $M = 1$  (equal mass) regime that has a narrow domain of attraction. If, instead, we had used either a large or small mass ratio, persistent motions may have been easier to achieve.

**Jumping on a Bridge.** As mentioned, the juggling model is like bouncing on a trampoline where the canvas has non-negligible mass. This is a situation one can perhaps imagine better by description of a real-world (if uncommon) situation we encountered on a wooden bridge about 3 m long. Both the existence and special nature of the solutions in this paper were demonstrated. This bridge had essentially only one vertical mode of oscillation that could be excited by jumping. After one jump in the air, with the bridge oscillating underneath, one generally would land with a bang as the oscillating bridge slapped up against one's descending feet. But jumping to just the right height one could jump almost as if on a massless trampoline, although one was really landing on a massive bridge. One had to jump just right initially, and then with concentration (but little physical effort), to repeat the smooth collision-free motions. The bridge would do about one and a half cycles of oscillation during the flight phase, as per the juggling theory here, and approximately match the downwards foot velocity at contact. If the timing got slightly off, a jarring collision would occur and one would have to start again.

**Posting on a Horse.** Also related is "posting" on a trotting horse where the motion of the horse is like a juggling "hand", and the rider's body is like a juggled ball. While posting, a rider uses some leg support on the stirrups perhaps for control and perhaps to reduce the effective gravity on the body. During the "flight" of the posting rider, the horse's back does about one and a half oscillations and then the rider has a gentle landing on the descending horse's back, like a juggled ball in the theory here. The phasing and motions are as per the juggling model, with the horse-back oscillations being analogous to a massive juggling "hand". Because the horse motion is forced and the horse mass high, posting is closer to a large or infinite  $M$ . Without any leg pressure, a person on a trotting horse has jarring collisions at twice the rate, i.e., at the same rate as the oscillations of the horse's back. This non-posting riding

on a trotting horse is perhaps close to the stable (dissipative) passive juggling in, for example, Schaal et al. (1996).

## 11. Discussion

**Relation to Open-loop Juggling.** The juggling model we have discussed above is an extreme case of an open-loop machine in that the open-loop controller has *no* actuation. The model is also catch-and-release in that there is sustained contact before each throw. Catch-and-release open-loop "Shannon" juggling is known to be strongly (deadbeat) stable (Schaal and Atkeson (1993)). Catch-and-release hopping, where the spring between the two masses is replaced with a displacement-controlled actuator, is similarly stable. But unlike the Shannon juggler, or a spring-less hopper, stability is an issue in our model because the hand has dynamics. (Similarly, our hopper has internal dynamics.)

In the limit as hand mass goes to infinity ( $M \rightarrow \infty$ ) the model presented here is equivalent to the catch-and-release juggler with a sinusoidal hand oscillation, at least for those cases where there is some sustained contact. For most values of launch, the return map approaches the identity line in this limit, not the horizontal line of a deadbeat system. The fact that in-flight perturbations of the juggled mass are totally quenched when hand mass is infinite is not revealed by our map, which allows only simultaneous perturbations of the hand and ball at the lift-off state.

**Existence of Persistent Motions Does Not Depend on the Value of  $e$ .** Note that the incessant hopping motions satisfy all the governing equations for any value of  $e$  (even  $e > 1$ ), not just  $e = 0$ . Off the periodic motions, the map and stability analysis do not apply for  $e \neq 0$ , but the catch-and-release constant-energy motions persist (are periodic solutions) for any value of  $e$  because the collisions are at zero relative velocity.

**Passive Stability and Dissipation.** There is a common intuition that dissipation is generally required for passive stability (see, for example, Schaal et al. (1996)). However this claim needs qualification.

In systems with non-holonomic contact (see, for example, Ruina (1998)) some care is needed in describing the role of dissipation for stability. In particular, stability does not depend on dissipation. Thus, the intuition based on experience with the vast library of holonomic mechanical systems—that stability depends on damping in general—is not correct. However, for systems whose only non-holonomicity comes from intermittent contact there are, despite claims to the contrary, no known systems that are entirely passive, non-dissipative and stable. Because of the 1D nature of the motions in this system, its intermittent contact is not non-holonomic (the system is essentially holonomic), these issues of holonomicity do not apply, and there is necessarily a need for dissipation to obtain stability.

But this does not mean that the desired motion is dissipative. A trivial example is a damped pendulum; it has no dissipation at its stable equilibrium. Dissipation is needed to attract, but no dissipation is needed *on* the stable motion.

Such is approximately the case for the system described in this paper (to the extent that the word “stable” is applicable). We have passive attraction to a dynamic limit cycle even though there is no energetic dissipation *on* the cycle. So the claim that dissipation is needed for stability is not negated here, but one should be aware that the stable motions themselves need not be dissipative.

Even if the hopping model were somehow expanded to two-dimensional running, where the non-holonomic issues are relevant, a model with a plastically-colliding massive foot will always have dissipation in some of its motions.

**Linear Stability is not Well Correlated with the Size of the Basin of Attraction.** With reference to Figure 8 it is interesting to note that, for this system at  $M = 1$ , with energy injection as a free structural parameter, the local basin of attraction (as defined earlier) is largest just when the linearized stability is lost. That is, a simple measure of the degree of stability is difficult here. The two obvious candidates, largeness of the local basin of attraction and smallness of the stability-governing eigenvalue, are negatively related to each other.

**Large Basin of Attraction for Extreme Values of  $M$ .** Figure 5(b) shows that for  $M = 1$  the attracting set to the special solution is extremely small. Furthermore, if the system is to be stabilized by unconditional injections of energy at each contact, these cannot be too large (as shown in Figure 8).

However, Figures 5(c) and (d) show that for sufficiently large *or* sufficiently small  $M$  any sufficiently large initial condition is attracted to one of the special motions. This attraction from arbitrary, but large enough, initial launches is easily verified with a dynamic simulator such as Working Model. That is, systems with  $M \gg 1$  or with  $M \ll 1$  find their own fixed points by marching forward in time from a large enough but arbitrary initial condition.

Taking into account that there is some dissipation besides the collision, with these extreme values of  $M$  genuine two-sided stability with a broad basin of attraction can be achieved by small injections of energy.

**Applicability.** Here we have described how the collision loss at the feet of a particularly simple hopping machine can be reduced by appropriate phasing of internal motions. The more general idea that the model exemplifies is that energetically-passive internal motions of a robot can be phased to minimize collision losses. Another example, mentioned in Kuo (2002a, 2002b) is the use of springs to reduce the step length, and hence the collisional loss, in walking. Finally, we do not claim that the passive collision-avoidance mechanism discussed here is, as literally presented, a means to great efficiency gains for legged locomotion (or juggling machines).

The presentation only shows in detail how the general idea works in a specific, and perhaps too-simple, implementation.

But the model does provide an example of the concept that proper phasing of passive internal degrees of freedom can be a means to reducing impact losses and thus improving energetic efficiency.

## 12. Conclusions

The work here extends the results of Schiehlen and Gao (Schiehlen 1987, Schiehlen and Gao 1989) by showing analytical conditions for lossless hopping, the symmetry of the solutions, the robustness to model perturbations, the identification with a simple model of juggling, the one-sided stability of the motions, the stabilization by small energy injections, and simple experimental verifications of the results.

In particular, collisional losses associated with a hopper’s foot impact (with any  $e < 1$ ) can be eliminated (in our simple model) by a passive retraction of the landing foot effected by a passive, possibly non-linear, spring. Similarly, in juggling, the ball–hand collision dissipation can be eliminated. Associated with this dissipation-free collision, for the case  $e = 0$ , is a periodic finite-amplitude motion that is one-way stable in theory, and can in practice be maintained and stabilized by tiny energy injections.

Lossless impact motions somewhat like those described here could be used to aid the efficiency and stability of hopping or juggling mechanisms. More generally, the example here shows that internal energy storage in a system can, if it has motions arranged to be appropriately synchronous with external collisions, lead to a decrease in net collisional dissipation.

## Acknowledgments

This work has been partly supported by the Department of Science and Technology, Government of India, and by a US National Science Foundation Biomechanics grant. Steve Collins helped set up and perform the air-track juggling experiment. The authors would like to thank Tony Bloch, Phil Holmes, Dan Koditschek and two anonymous reviewers for comments on the text. Closely related work was done independently and simultaneously to this by Patrick Haggerty in “Radiation-Induced Instability,” PhD Thesis, University of Michigan, 2001.

## References

- Ahmadi, M., and Buehler, M. 1997. Stable control of a simulated one-legged running robot with hip and leg compliance. *IEEE Trans. Robot. Autom.* 13(1):96–104.
- Alexander, R. M. 1977. Mechanics and scaling of terrestrial locomotion, *Scale Effects in Animal Locomotion*, ed. T.J. Pedley, 93–110. London: Academic Press.

- Alexander, R. M. 1990. Three uses for springs in legged locomotion. *Int. J. Robot. Res.* 9(2):53–61.
- Berkemeier, M., and Desai, K. 2002. A comparison of three approaches for the control of hopping height in legged robots. *Int. J. Robot. Res.* at press.
- Blajer, W., and Schiehlen, W. 1992. Walking without impacts as a motion/force control problem. *ASME J. Dyn. Syst. Meas. Control* 114:660–665.
- Brown, B., and Zeglin, G. 1998. Control of a bow leg hopping robot, *IEEE Int. Conf. on Robotics and Automation* 1:793–798.
- Buehler, M., and Koditschek, D. E. 1990. From stable to chaotic juggling: Theory, simulation, and experiments, *IEEE Int. Conf. on Robotics and Automation* Cincinnati, OH, 1976–1981.
- Buehler, M., Koditschek, D. E., and Kindlmann, P. J.. 1994. Planning and control of robotic juggling and catching tasks. *Int. J. Robot. Res.* 13(2):101–118.
- Canudas de Wit, C., Roussel, L., and Goswami, A. 1997. Periodic stabilization of a 1-DOF hopping robot under non-linear compliant surface. *Proc. IFAC Symposium on Robot Control SYROCO*, Nantes, France, 405–410.
- Chatterjee, A., and Garcia, M. 2000. Small slope implies low speed for McGeer's passive walking machines. *Dyn. Stab. Syst.* 15(2):139–157.
- Francois, C., and Samson, C. 1994. Running with constant energy. *IEEE Int. Conf. on Robotics and Automation*, 1:131–136.
- Goldhirsch, I., Noskowitz, S. H., and Schuss, Z. 1993. Band-edge localization as intermittent chaos. *Phys. Rev. B* 47:1918–1935.
- Koditschek, D. E., and Buehler, M. 1991. Analysis of a simplified hopping robot. *Int. J. Robot. Res.* 10(6):587–605.
- Kuo, A. D. 2002. Energetics of actively powered locomotion using the simplest walking model. *ASME J. BME* 124:113–120.
- Lapshin, V. V. 1992. Vertical and horizontal motion control of a one-legged hopping machine. *Int. J. Robot. Res.* 11(5):491–498.
- M'Closkey, R. T., Vakakis, A. F., and Burdick, J. W. 1990. On the periodic motions of a simple hopping robot. *IEEE Int. Conf. on Systems, Man and Cybernetics*, 771–777.
- McGeer, T. 1990. Passive bipedal running. *Proc. R. Soc. B* 240(1297):107–134.
- Michalska, H., Ahmadi, M., and Buehler, M. 1996. Vertical motion control of a hopping robot. *IEEE Int. Conf. on Robotics and Automation*.
- Rad, H., Gregorio, P., and Buehler, M. 1993. Design, modeling and control of a hopping robot. *IEEE/RSJ Conf. Intelligent Robots and Systems*, Yokohama, Japan, 1778–1785.
- Raibert, M. H. 1986. *Legged Robots that Balance*. Cambridge, MA: MIT Press.
- Reddy, C. K., and Pratap, R. 2002. Multimodal Map and Complex Basin of Attraction of a Simple Hopper, submitted.
- Ruina, A. 1998. Non-holonomic stability aspects of piecewise-holonomic systems. *Rep. Math. Phys.* 42(1/2):91–100.
- Schaal, S., and Atkeson, C. G. 1993. Open loop stable control strategies for robot juggling. *IEEE Int. Conf on Robotics and Automation* 3:913–918.
- Schaal, S., Sternad, D., and Atkeson, C. G. 1996. One-handed juggling: A dynamical approach to a rhythmic movement task. *J. Motor Behav.* 28(2):165–183.
- Schiehlen, von Herausgegeben W. 1987. Vortragsreihe zum 75. Geburtstag von Kurt Magnus (in German).
- Schiehlen, W., and Gao, J. 1989. Simulation des stoßfreien hüpfens. *ZAMM, Z. Angew. Math. Mech.* 69:302–303 (in German).
- Sternad, D., Duarte, M., Katsumata, H., and Schaal, S. 2000. Dynamics of a bouncing ball in human performance. *Phys. Rev. E* 63:011902-1–011902-8.
- Vakakis, A. F., and Burdick, J. W. 1990. Chaotic motions in the dynamics of a hopping robot. *IEEE Int. Conf. on Robotics and Automation* 3:1464–1469.
- Wei, Terence E., Nelson, Gabriel M., Quinn, Roger D., Verma, Hiten, and Garverick, Steven L. 2000. Design of a 5-cm monopod hopping robot. *Proc. IEEE Int. Conf. on Robotics and Automation*.
- Zavalo-Rio, A., and Brogliato, B. 1999. On the control of a one degree-of-freedom juggling robot. *Dyn. Control* 9(1):67–91.
- Zeglin, G., and Brown, B. 1998. The bow leg hopping robot. *IEEE Int. Conf. on Robotics and Automation* 1:781–786.